SEVILLE 2023
7th International Seminar on O.R.C. Power Systems

DOI: https://dx.doi.org/10.12795/9788447227457_129

ASSESSMENT OF HIGH TEMPERATURE HEAT PUMP LAYOUTS EQUIPPED WITH A BLADELESS TURBOEXPANDER

Matteo Passalacqua[1,*], Simone Maccarini[1], Stefano Barberis[1], Alberto Traverso[1]

[1]*Thermochemical Power Group, University of Genova, Via Montallegro 1, 16145 Genova, Italy*

*Corresponding Author: matteo.passalacqua@edu.unige.it

ABSTRACT

Efficient and resilient reverse cycles at MW-scale are needed in industry and energy communities for pursuing the ambitious targets of electrification of industrial processes and thermal generation via renewable power.
This work evaluates the optimal thermodynamic performance features of heat pump cycles comparing conventional layouts with those adopting a Tesla turboexpander, for recovering pressure drop in high temperature applications. The paper focuses on n-pentane (R601), a natural refrigerant, being a favorable substitute of synthetic refrigerants thanks to its low global warming potential (GWP) and adequate thermophysical properties that could allow to reach high temperature thermal outputs (>150°C), thus, being suitable for some specific industrial processes. Tesla or bladeless turboexpanders are a promising technology for small volumetric flows and two-phase fluids, featuring low sensitivity to downscaling effects, while retaining high rotor efficiency, which is being investigated for energy-harvesting solutions. The benefit of introducing such expansion device in place of a conventional lamination valve is assessed, in different layout configurations. Simulations were conducted using an improved version of WTEMP-EVO modeling tool, proprietary to University of Genoa.
Results show that the use of Tesla expander improves significantly the overall thermal efficiency in terms of coefficient of performance (COP), thanks to power recovered, depending on the cycle layout.

1 INTRODUCTION

The continuous increase of GHG emissions, in particular carbon dioxide that reached a world record in 2022, is encouraging many sectors to adopt new strategies to reduce emissions. Transport, buildings, and industry are the most relevant sectors in terms of final energy consumption, about 2.9 Gtoe each for a total of 60% (IPCC, 2021).
The course of action to abate pollutant substances and GHG emission includes the electrification of heating systems, both industrial and DHNs, which together account for roughly 30% the total emission (IPCC, 2021). However, a benefit from electrification is only obtained if electricity is produced mostly from renewable sources (e.g., solar photovoltaic, concentrated solar power, wind power, hydro, biomass) or carbon-free energy carriers (green hydrogen and green ammonia).
From this point of view, heat pumps are a promising solution. The latest research has focused mainly on three aspects of heat pump plants, namely plant design and machinery optimization, expander introduction, high temperature heat pumps (HTHP) applications and the use of low-GWP natural refrigerants. Recent literature contains numerous studies on heat pumps performance assessment and the replacement of inefficient heating systems with such technology (Adamson et al., 2022) (Chen et al., 2022) (Pan et al., 2021) (Dai et al., 2020) (Jibran et al., 2022).. Working fluids for reverse cycles typically feature high specific heat, high latent heat of vaporization. Halogenated hydrocarbons, such as hydrofluorocarbons (HFCs) and hydrochlorofluorocarbons (HCFCs) are employed at present in many heat pump plants. In accordance with Montreal Protocol (Montreal Protocol, 1987), Kyoto Protocol (Kyoto Protocol, 1997) and the successive Kigali Amendment (Kigali Amendment, 2019) there is an evident need for reducing their usage.

Organic working fluids are a promising alternative to of synthetic refrigerants since they have low GWPs while showing comparable thermophysical properties. Besides, some of them allow to achieve high heat sink temperatures thanks to their high critical temperature, interesting for a variety of different industrial application. The recent scientific research focused on natural and low-GWP refrigerants performance (Meinel, Wieland and Spliethoff, 2014) (Kumar Saini et al., 2021) as well as comparative reviews (Bamigbetan et al., 2017) (Frate, Ferrari and Desideri, 2019). A promising example is n-pentane (R601): in accordance with several literature sources (Arpagaus et al., 2018) (Wu et al., 2020), with the relevant exception of water (R718), it has the highest expected COP in the typical temperature range of HTHPs. Some authors (Arpagaus et al., 2018) perform a widespread analysis on several heat pump working fluids, including n-pentane, to evaluate the most suitable ones for high heat sink temperatures. They found that such hydrocarbon is outperformed in terms of optimal temperature range by water and R1336mzz(Z) only. Their results show that R601 is among the most efficient fluids in the range 130-160°C of heat sink temperatures, topping out at a COP of 3.27 for a temperature lift of 70 K. Other authors (Sulaiman et al., 2022) compare different low-GWP refrigerants for HTHP application, showing that R601 has 4% to 18% lower power consumption compared to R245fa. Besides, TEWI for R601 is around 27% lower. Very little literature is available specifically on n-pentane heat pumps. In an old work (Yamazaki and Kubo, 1985), researchers evaluated a 400 kW R601 layout supplying steam at 130°C from waste heat at 90°C. They obtained a COP of 4.5 for source and sink temperatures of 80°C and 135°C, respectively.

The introduction of a dynamic expander in reverse cycles as an energy harvesting device is covered in literature (Zhang et al., 2013) (Nickl et al., 2005) and the performance improvements are registered between 10% and 30% with respect to the base cycle, depending on the layout characteristics (Murthy et al., 2019). Multidisc bladeless friction turboexpanders, also known as Tesla turbines (Tesla, 1913), represent a promising technology as small-scale machinery due to their low sensitivity to downscaling effects, retaining high rotor efficiency. Some authors performed a systematic loss characterization (Renuke et al, 2022), showing that the largest contributions reside in stator-rotor interaction (40%) and ventilation (15%) losses, followed by leakages. Nowadays, its ability to handle low volumetric flows, including two-phase fluids, may pave the way towards Tesla expander adoption in heat pumps as COP booster. In general, this paper aims to widen the knowledge on such an innovative and effective solution to emissions reduction.

2 METHODS

2.1 Layouts analysed

This work assesses different layouts of n-pentane reverse cycles, firstly comparing performance of simple expansion cycle with a novel layout featuring a Tesla turboexpander, and secondly evaluating to what extent two stage compression is beneficial.

Figures 1a-1d describe the investigated layouts: for each of them, models of physical components are created and interfaced with each other to assemble complete cycles.

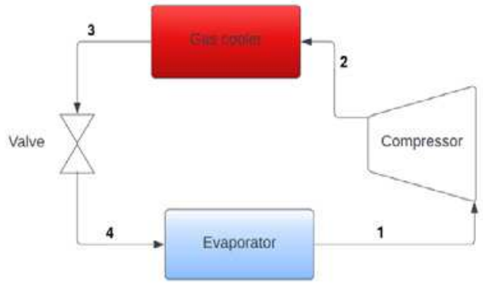

a)

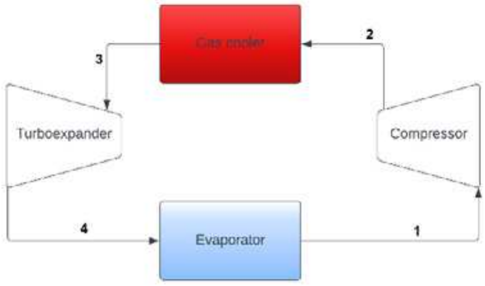

b)

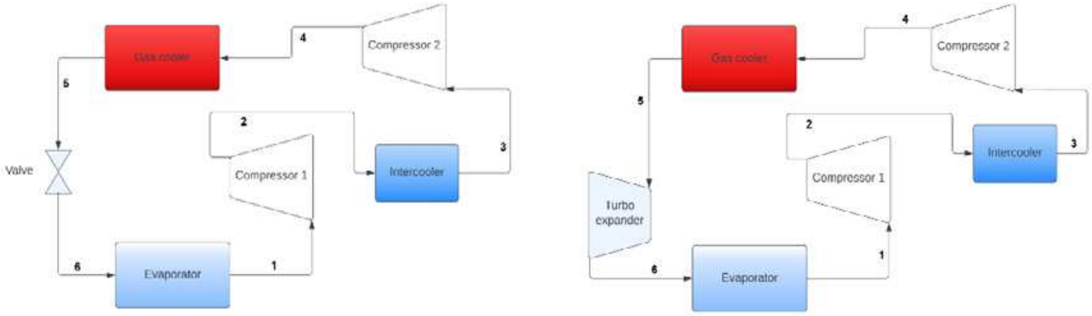

c) **d)**

Figure 1a-1d – Schematics of investigated layouts

2.2 Thermodynamic Modelling

This section describes the underlying principles behind the M physical component models constituting the system. The simulation program WTEMP-EVO has been devised to assess and enhance the techno-economic effectiveness of various cycle arrangements and can evaluate several pure fluids with a two-phase or real-gas nature via the utilization of CoolProp (Bell et al., 2014) thermodynamic libraries. This is, in essence, an expansion of WTEMP (Traverso et al., 2004) retaining its modular approach, implying that every component is depicted by a subroutine that calculates parameters based solely on basic thermal evaluations performed within each component, independently of the other constituents. This numerical approach permits the components to be interlinked to obtain the evaluation of any preferred layout. Most component models are lumped representations of real components, with the exception of heat exchangers, which are modelled as 1D components, discretized in 30 computation sections. All components are adiabatic, thus, heat losses towards the environment are neglected.

The compressor reproduces the real component in the plant configuration. Equation (1) reports the definition of polytropic efficiency used in this work for such component. Here, β is the compression ratio, k is the specific heat ratio ($k = c_p/c_v$) and m the exponent of the polytropic transformation. Equation (2) highlights the link between isentropic efficiency and polytropic exponent.

$$\eta_{pol} = \frac{m}{m-1} \cdot \frac{k-1}{k}, \quad (1)$$

$$\eta_c = \frac{1-\beta^{\frac{k-1}{k}}}{1-\beta^{\frac{m-1}{m}}} \quad (2)$$

$$h_{out,turb} = h_{in,turb} - (h_{in,turb} - h_{out,s,turb}) \cdot \eta_{s,turb} \quad (3)$$

The turboexpander operates an expansion of the working fluid, generating power at the shaft. This component was assessed by means of equation (3).

The modelling of the expansion valve simply considers an isoenthalpic process between inlet and outlet.

The heat exchanger model refers to a shell and tube heat exchanger. The modeling is based on a counter-flow rationale, with the user setting a primary temperature or quality and other parameters such as approach, pinch point temperature difference, and pressure losses. The results of the thermodynamic cycle are then used to determine the geometrical characteristics of the heat exchanger, for which inputs include the velocities of the working and source fluids (u_{fluid} and u_{source}), as well as the internal and external diameters of the pipes (D_{int} and D_{ext}). The heat transfer is computed by use of the *ε-NTU* criterion, as suggested by notable works (Incropera et al., 2010).

The heat exchanger is discretized into a number of cells (N=30 for this work) assuming a constant overall heat transfer coefficient for each cell. The convective heat transfer coefficient is calculated for each cell. The product *UA* is then calculated by assessing the effectiveness ε for each cell. This involves assuming equal thermal power exchange for each cell and comparing the actual enthalpy drop of the fluid to the enthalpy drop experienced by the fluid with the lowest heat capacity. The heat transfer surface area is then determined for each cell and summed up to calculate the total surface area of the heat exchanger. It should be noted that thermal conduction along the axial coordinate within the piping material is disregarded in the analysis.

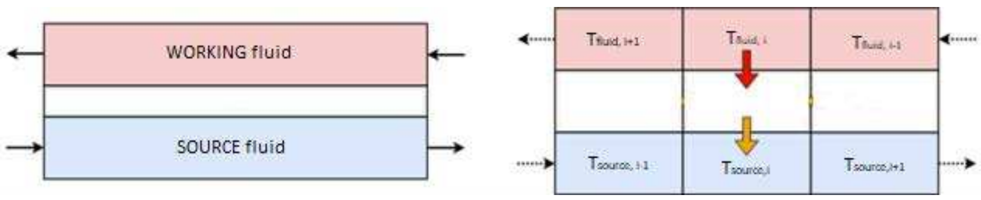

Figure 2: Scheme of counter-flow heat exchanger (cooler)

3 SIMULATION AND RESULTS

3.1 Model Inputs and Constraints

This section describes the model inputs and main constraints. A size of 1 MW_{heat} heating power was chosen as a reference of a sizeable heat pump plant. Table 1 contains the boundary conditions and the general assumptions for each component of the cycle.

Table 1: Boundary conditions and general assumptions

BCs and General Assumptions	
Working fluid	R601
Reference size (Q_{heat})	1 MW_{heat}
Heat exchanger pressure loss	3%
Thermal loss towards ambient	Neglected
Max compressor outlet temperature	180 °C
ΔT superheating (compressor inlet)	50 °C
ΔT subcooling (expander inlet)	30 °C
Condensation pressure (reference)	20 bar
Evaporation pressure (reference)	0.8 bar
Minimum ΔT at HXs	5 K
Mechanical efficiency	0.85
Electrical efficiency	0.9
Compressor polytropic efficiency	0.91
Tesla turbine isentropic efficiency	0.44

It is worth noting that a polytropic compressor efficiency was assumed, according to the assumptions in Table 1. In addition, a maximum temperature of the cycle, that is the compressor outlet temperature, was chosen (Table 1). The justification for this choice is two-fold. On the one hand, high temperatures lead to thermal decomposition of the compressor lubricant, which should be avoided. On the other hand, operation near the critical temperature of R601 (196°C) should be avoided for thermodynamic reasons, such as high variability of the specific heat around the critical point. In addition, such temperature is adequate to ensure sufficient heat transfer even at very high heat sink temperatures. This choice is in line with previous studies (Frate, Ferrari and Desideri, 2019) (Ommen et al., 2015).

3.2 Parametric analysis

The COP is defined as usual for heat pumps, that is, by the following equations:

$$COP_{HP} = \frac{\dot{Q}_{heat}}{\dot{W}_{elect}} \quad (3)$$

A parametric analysis exploring different key parameters was conducted, both for the simple cycle (Figures 3a-3c) and for the Tesla modified cycle (Figures 4a-4c).

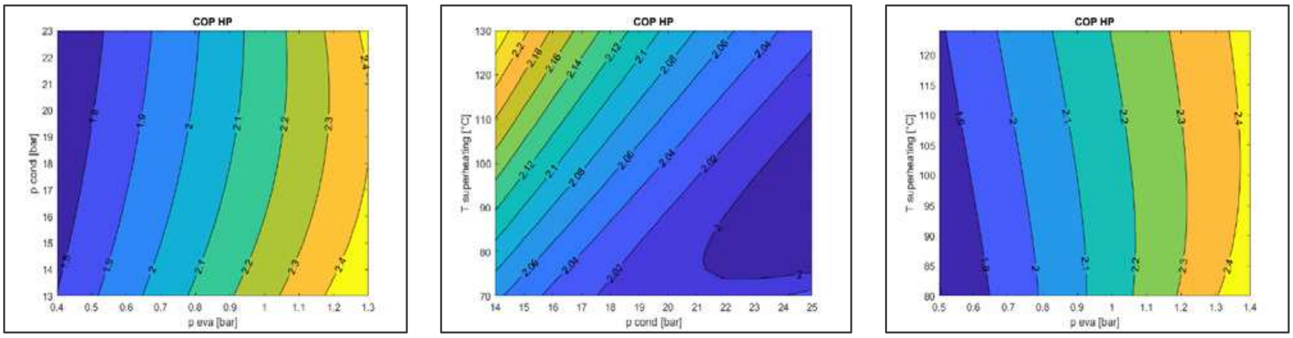

a) **b)** **c)**

Figure 3a-3c: COP sensitivity against a) p_{cond}/p_{eva}, b) T_{sh}/p_{cond} and c) T_{sh}/p_{eva} for simple cycle

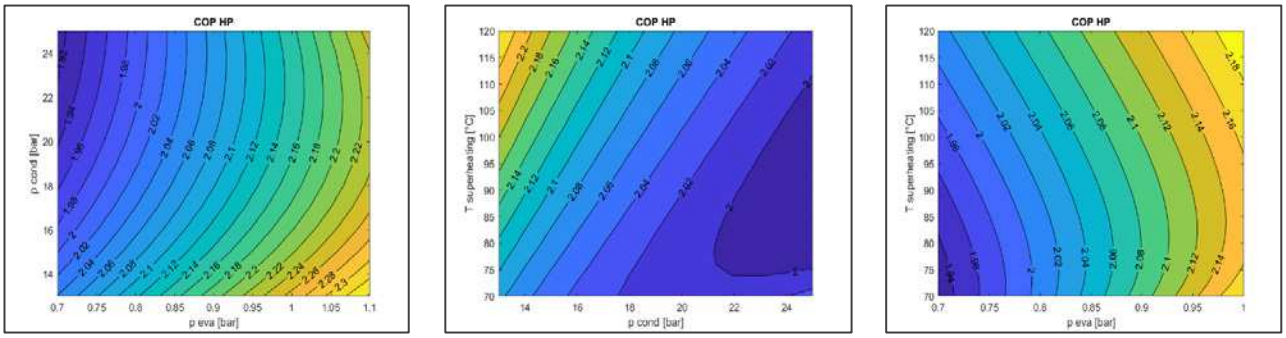

a) **b)** **c)**

Figure 4a-4c: COP sensitivity against a) p_{cond}/p_{eva}, b) T_{sh}/p_{cond} and c) T_{sh}/p_{eva} for Tesla cycle

Figure 3a demonstrates that COP of the heat pump is scarcely sensitive to condensation pressure, while highly depends on evaporation pressure. Figure 3b depicts an increasing heat pump performance with increasing superheating temperature (i.e., compressor inlet temperature) at low condensation pressures, and Figure 3c show that evaporation pressure have a negligible influence on the COP value. For the Tesla modified cycle, trends depicted are similar, with performance values varying less but in accordance with a narrower pressure range on horizontal axis.
It should be noted that the superheating temperatures are consistently higher than the saturation temperatures at evaporating pressures, confirming that dry refrigerants require high degree of superheating before compressor inlet. In addition, dry refrigerant may not benefit from two-stage compression, or the efficiency gain is very marginal, as shown in previous literature (Meinel, Wieland and Spliethoff, 2014).
Figures 5a to 5c display the required compressor thermodynamic power. With reference to equation (4), the trends are in line with the COP plots.

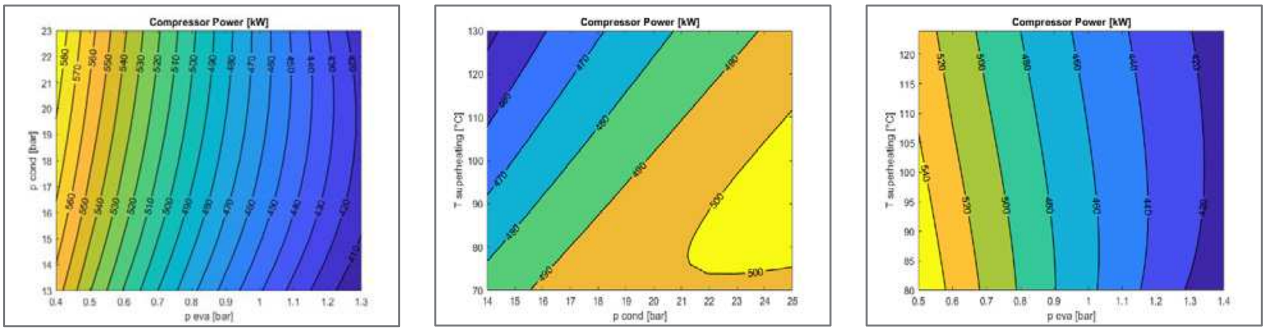

a) **b)** **c)**

Figure 5a-5c: Compressor power against a) p_{cond}/p_{eva}, b) T_{sh}/p_{cond} and c) T_{sh}/p_{eva}

With the purpose of addressing energy harvesting, the available expansion power for the Tesla expander is depicted in Figures 6a-6c. It may be observed that such power is slightly dependent on condensation pressure, while increases with decreasing evaporation pressure and superheating temperature.
Figure 7 highlights the COP improvement for three values of evaporation pressure, assuming constant condensation pressure (20 bar). The percentage difference is defined as the difference between Tesla cycle COP and simple cycle COP, divided by the simple cycle COP. The evaporation pressures reported in Figure 7 correspond to R601 saturation temperatures of 16.8 °C, 29.8 °C and 35.7 °C, respectively.

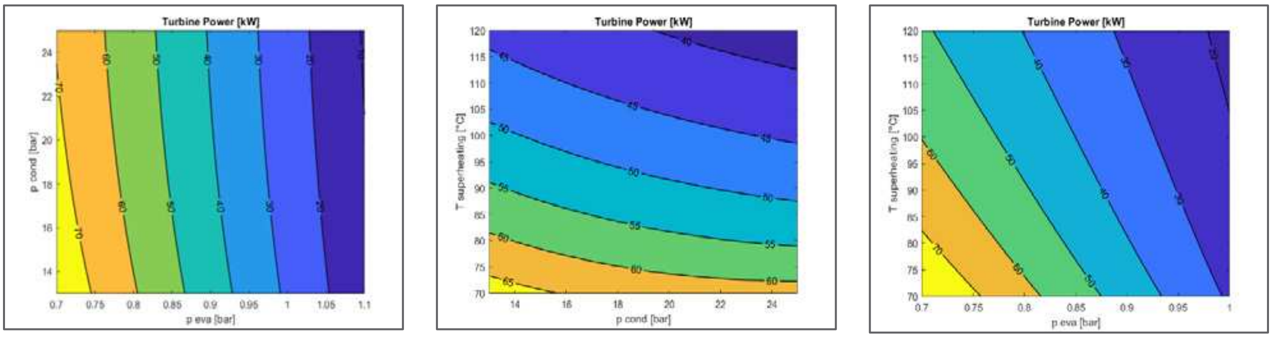

a) **b)** **c)**

Figure 6a-6c: Tesla expander available power against a) p_{cond}/p_{eva}, b) T_{sh}/p_{cond} and c) T_{sh}/p_{eva}

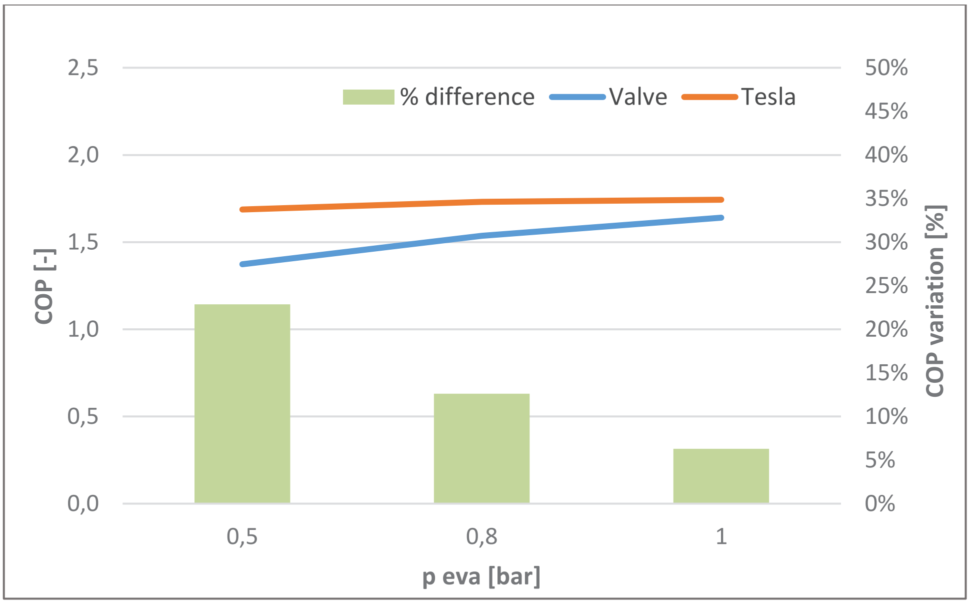

Figure 7: COP comparison between simple and Tesla modified cycle (p_{cond} = 20 bar)

4 PROPOSED CASE STUDY

Despite being a very promising energy recovery option, low-temperature waste heat has major challenges associated with its recovery. Moreover, heat pump performance is always reduced when heat upgrade requires high temperature lifts. To further improve the knowledge of HTHP technology, a real industrial case study is presented below. These results might indicate the suitability of HTHP for various industrial applications and justify further detailed research and experimental activities.

4.1 Case Study Description

A manufacturer of laminate products for the building and furniture industry disposes of a hot water tank from the pressing process, that is to be evaluated as a thermal source for the production of pressurized hot water at 160°C and 20 bar for a different process.
Since a consistent temperature glide is involved (around 100 °C, Table 2), R601 was evaluated due to its favourable properties. Machinery efficiencies are the same reported in Table 1.

Table 2: Boundary conditions for the case study

BCs and General Assumptions	
Source water inlet temperature	≈ 60 °C
Source water outlet temperature	≈ 35 °C
Process water inlet temperature	≈ 120 °C
Process water outlet temperature	160 °C

4.2 Case Study Results

Table 3 delivers briefly the results of the simulation for the aforementioned industrial case study.

Table 3: Performance comparison for R601 HTHP according to the case study

COP comparison	
COP simple cycle	1.54
COP Tesla modified cycle	1.73

As expected, the heat pump performance benefits from the presence of a Tesla expander by matter of 13%, in good accordance with numerous literature sources. To complete the analysis, Figures 8a-8b report p-h charts for the two cases and Figures 9a and 9b show examples of T-Q chart along the discretization coordinate x relative to two relevant heat exchange processes for the case study conditions. Figure 8a refers to the de-superheating process of the refrigerant prior to its condensation.

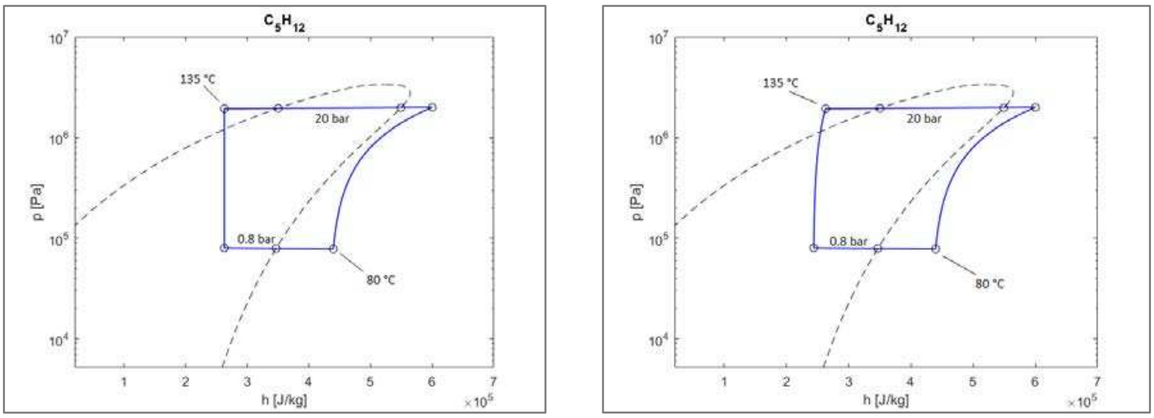

a) b)

Figure 8a-8b: Semi-logarithmic p-h comparison for R601 HTHP according to the case study

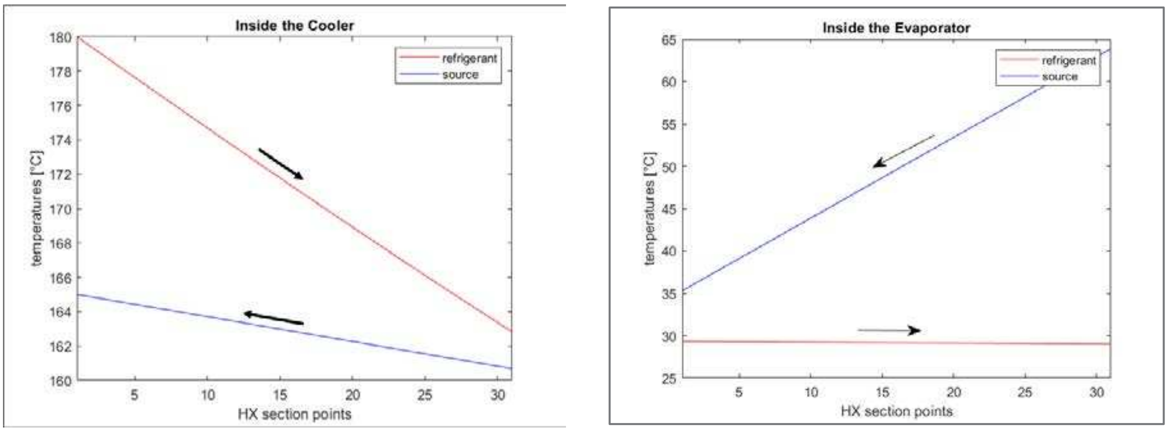

a) b)

Figure 9a-9b: T-x chart for the a) de-superheating and b) evaporation according to the case study (x represents the axial coordinate of the external heat transfer fluid)

5 CONCLUSIONS

In this paper, techno performance of n-pentane HTHP have been analysed. A MW-sized plant was investigated as reference for an industrial application. The updated WTEMP-EVO software was adopted to model and simulate the cycle. Performance was assessed under on-design conditions and a sensitivity analysis on relevant parameters was performed.

The results confirm the promising use of expanders to harvest a significant amount of energy and to improve the COP of the cycle. Optimal conditions for turboexpander cycle are obtained in a narrower range of operating conditions. A 13% COP improvement was achieved in the industrial case study simulation. In addition, Tesla turbines have further advantages concerning almost size-independent efficiency and reduced cost with respect to traditional turboexpanders, and potentially can better manage two-phase flows, without the risk of erosion. Dual stage compression cycles were not assessed, since R601 is a dry refrigerant and, having a very sloped saturation curve, compression “follows” that curve quite solidly (Figures 6a-6b), so fluid intercooling may not improve significantly cycle performance, considering also the added plant complexity and costs.

NOMENCLATURE

COP	Coefficient of Performance
GHG	Greenhouse Gas
GWP	Global Warming Potential
HP	Heat Pump
HTHP	High Temperature Heat Pump
IPCC	Intergovernmental Panel on Climate Change
NTU	Number of Transfer Units
TEWI	Total Equivalent Warming Impact
UNFCC	United Nations Framework Convention on Climate Change

Symbols

P	Pressure	[bar]
T	Temperature	[°C, K]
h	Enthalpy	[kJ/kg]
s	Entropy	[kJ/kg K]

m	Mass flow	[kg/s]
x	HX discretization coordinate	[-]
ΔT	Temperature gradient	[K]
β	Pressure ratio	[-]
k	Heat capacity ratio	[-]

Subscript

in	Inlet
out	Outlet
int	Internal
ext	External
elect	Electrical
s	Isentropic
pol	Polytropic
cond	condenser
eva	evaporator
sh	Superheating
subc	Subcooling
fluid	Working fluid
source	Source fluid
heat	Heating power

REFERENCES

Adamson, K.M, et al., 2022, "High-temperature and transcritical heat pump cycles and advancements: A review,." *Renewable and Sustainable Energy Reviews*.

Arpagaus, C., Bless, F., Uhlmann, M., Schiffmann, J. and Bertsch, S.,2018, High temperature heat pumps: Market overview, state of the art, research status, refrigerants, and application potentials, *Energy* 152, 985-1010.

Bamigbetan, O., Trygve, M.E., Neska, P., and Bantle, M., 2017, Review of vapour compression heat pumps for high temperature heating using natural working fluid, *International Journal of Refrigeration* 80, 197-211.

Bell, I., Wronski, J., Quoilin, S., and Lemort, V., 2014, Pure and pseudo-pure fluid thermophysical property evaluation and the open-source thermophysical property library CoolProp, *Ind Eng Chem Res* 53, 2498-2508.

Bergman, T.L., Lavine, A., Incropera, F. and DeWitt, D., 2018, *Fundamentals of Heat and Mass Transfer, 8th Edition.* Wiley & Sons.

Chen, Y., Standl, P., Weiker, S., and Gaderer, M., 23022, A general approach to integrating compression heat pumps into biomass heating networks for heat recovery, *Applied Energy* 310.

Dai, B., Qi, H., Dou, W., Liu, S., Zhong, D., Yang, H., Nian, V. and Hao, Y., 2020, Life cycle energy, emissions and cost evaluation of CO2 air source heat pump system to replace traditional heating methods for residential heating in China: System configurations, *Energy Conversion and Management* 218.

European Fluorocarbons Technical Committee, https://www.fluorocarbons.org/environment/climate-change/global-warming-potential/ (accessed November 30, 2022).

Ferrando, M., Renuke, A., Traverso, A. and Sishtla, V., 2021, A new design method for two-phase nozzles in high efficiency heat pumps, *International Journal of Refrigeration*, 148-156.

Frate, G.F, Ferrari, L. and Desideri, U., 2019, Analysis of suitability ranges of high temperature heat pump working fluids, *Applied Thermal Engineering*, 628-640.

IPCC, Sixth Report Assessment (AR6), Geneva (CH), 2021.

Jibran, M., Zuberi, S., Hasanbeigi, A. and Morrow, W., 2022, Bottom-up assessment of industrial heat pump applications in U.S. Food manufacturing, *Energy Conversion and Management* 272.

Kigali Amendment, Kigali, 2019.
Kyoto Protocol, Kyoto, 1997.
Meinel, D, Wieland, C. and Spliethoff, H., 2014, Effect and comparison of different working fluids on a two-stage ORC concept, *Applied Thermal Engineering*, 246-253.
Montreal Protocol, Montreal, 1987.
Murthy, A.A, Subiantoro, A., Norris, S., and Fukuta, A., 2019, A review on expanders and their performance in vapour compression refrigeration systems, *International Journal of Refrigeration* 106, 427-446.
Nickl, J., Will, G., Quack, H., and Kraus, W.E., 2005, Integration of a three-stage expander into a CO2 refrigeration system, *International Journal of Refrigeration* 28, no. 8, 1219-1224.
Ommen, T, Jensen, J.K., Markussen, W.B., Reinholdt, L., and Elmegaard, B., 2015, Technical and economic working domains of industrial heat pumps: Part 1 – Single stage vapour compression heat pumps, *International Journal of Refrigeration*, 168-182.
Pan, M., Zhu, Y., Liang, Y., Lu, F., Zhi, R., and Xiao, G., 2021, Performance assessment of a waste-heat driven CO2-based combined power and refrigeration cycle for dual-temperature refrigerated truck application, *Energy Conversion and Management* 249, no. 114863
Renuke, A., Reggio, F., Traverso, A., and Pascenti, M., 2022, Experimental Characterization of Losses in Bladeless Turbine Prototype, *Journal of Engineering for Gas Turbines and Power,* 144.
Renuke, A., and Traverso, A., 2022, Performance assessment of Tesla expander using Three-Dimensional numerical simulation, *Journal of Engineering for Gas Turbines*, 144, no. 11
Sarbu, I. 2014, A review on substitution strategy of non-ecological refrigerants from vapour compression-based refrigeration, air-conditioning and heat pump systems, *International Journal of Refrigeration* 46, 123-141.
Sulaiman, A., Cotter, D.F., Le, X.K., Huang, M.J., and Hewitt, N.J., 2022, Thermodynamic analysis of subcritical high temperature heat pump using low GWP refrigerants: A theoretical evaluation, *Energy Conversion and Management* 268.
Tesla, N., Turbine. U.S. Patent 1061206, 1913.
Traverso, A. Reverse cycle machine provided with a turbine. Patent WO2018127445A1
Traverso, A., A.F Massardo, Cazzola, W. And Lagorio, G., 2004, WIDGET-TEMP: a novel web-based approach for thermoeconomic analysis and optimization of conventional and innovative cycles, *ASME Turbo Expo 2004: Power for Land, Sea, and Air,* 623-631.
UNFCCC. Paris Agreement, Paris, 2015.
Westphalen, D., and Dieckmann, J., 2004, Scroll Expander for Carbon Dioxide Air Conditioning Cycles, *International Refrigeration and Air Conditioning Conference.* Purdue, IN (US).
Wu, D., B Hu, Wang, R.Z., Fan, H., and Wang, R., 2020, The performance comparison of high temperature heat pump among R718 and other refrigerants, *Renewable Energies*, 715-722.
Yamazaki, T., and Kubo, Y., 1985, Development of a high-temperature heat pump, *IEA Heat Pump Centre Newsletter* 3, no. 4, 18-21.
Zhang, Z., Yitai M., Li, M., and Li Z., 2013, Recent advances of energy recovery expanders in the transcritical CO2 refrigeration cycle, *HVAC&R Research* 19, no. 376-384.